caspus engineering
analysis | simulation | design

CFD METHODOLOGY FOR SIMULATION OF LNG SPILLS AND RAPID PHASE TRANSITION (RPT)

Dr Andrei Horvat

Caspus Engineering

Didcot, April 2019

Content

Introduction

Scenario description

Liquid layer dynamics

Boiling regimes and rapid phase transition (RPT)

Dispersion

CFD simulation results and discussion

Further challenges and conclusions

Introduction

The simulation methodology specifically developed for a mainstream commercial CFD toolset:

- behaviour of LNG spills from their initial release
- spreading on the water surface
- Rapid Phase Transition (RPT)
- subsequent dispersion

Robustness of the combined approach is unique!

Introduction

A complex release scenario in a framework of a commercial project - an LNG spill between FLNG vessel and LNG carrier

- calculate the size of the flammable cloud
- determine the resulting overpressure due to an RPT event

Particular interest for deterministic risk assessment in the expanding LNG sector

Introduction

Project results used in a highly selective manner

- demonstrates modelling principles
- avoids commercial sensitivity of specific findings

Scenario description

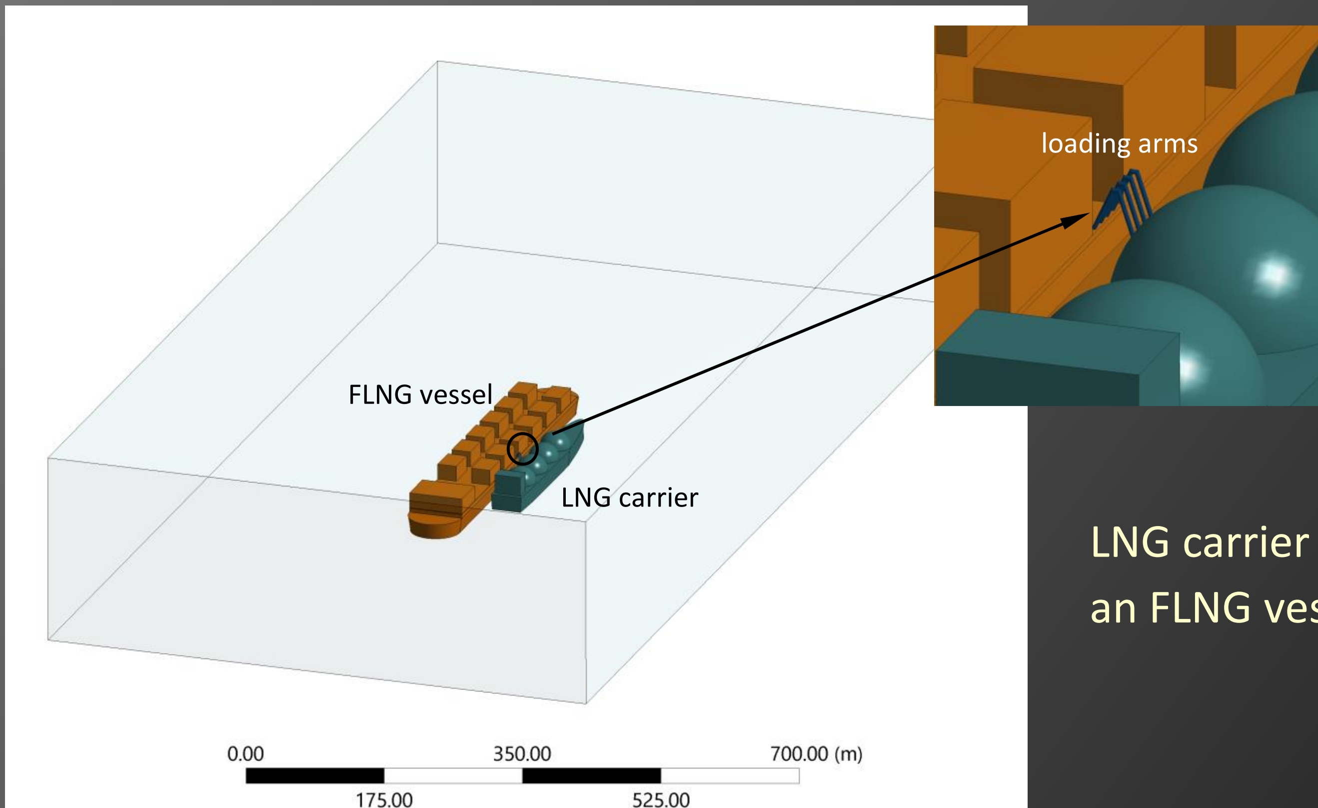

LNG carrier moored alongside an FLNG vessel

- Proximity of both vessels - shape and propagation rate of the LNG layer, and the subsequent gaseous cloud
- Failure in the FLNG process train with an LNG release rate of 1020 kg/s and the duration of 76.2 s

Scenario description

- Agreed LNG composition: CH_4 - 78.76, C_2H_6 - 12.31 and C_3H_8 - 8.93 mass %
- The sea and air temperature set to 25°C, with the wind speed of 0.5 m/s at the reference height of 50 m

Liquid layer dynamics

Dispersion simulations

- prediction of cloud behaviour
- large simulation domains

Liquid layer

- just few millimetres thick
- very fine grid spacing needed

Local liquid surface instabilities

- small time-steps required

These constrains make such CFD simulations prohibitively expensive!

solution →

2D approximation of the liquid layer coupled to a larger, 3D ambient domain for dispersion analysis

Liquid layer dynamics

General purpose CFD codes require multiphase formulation

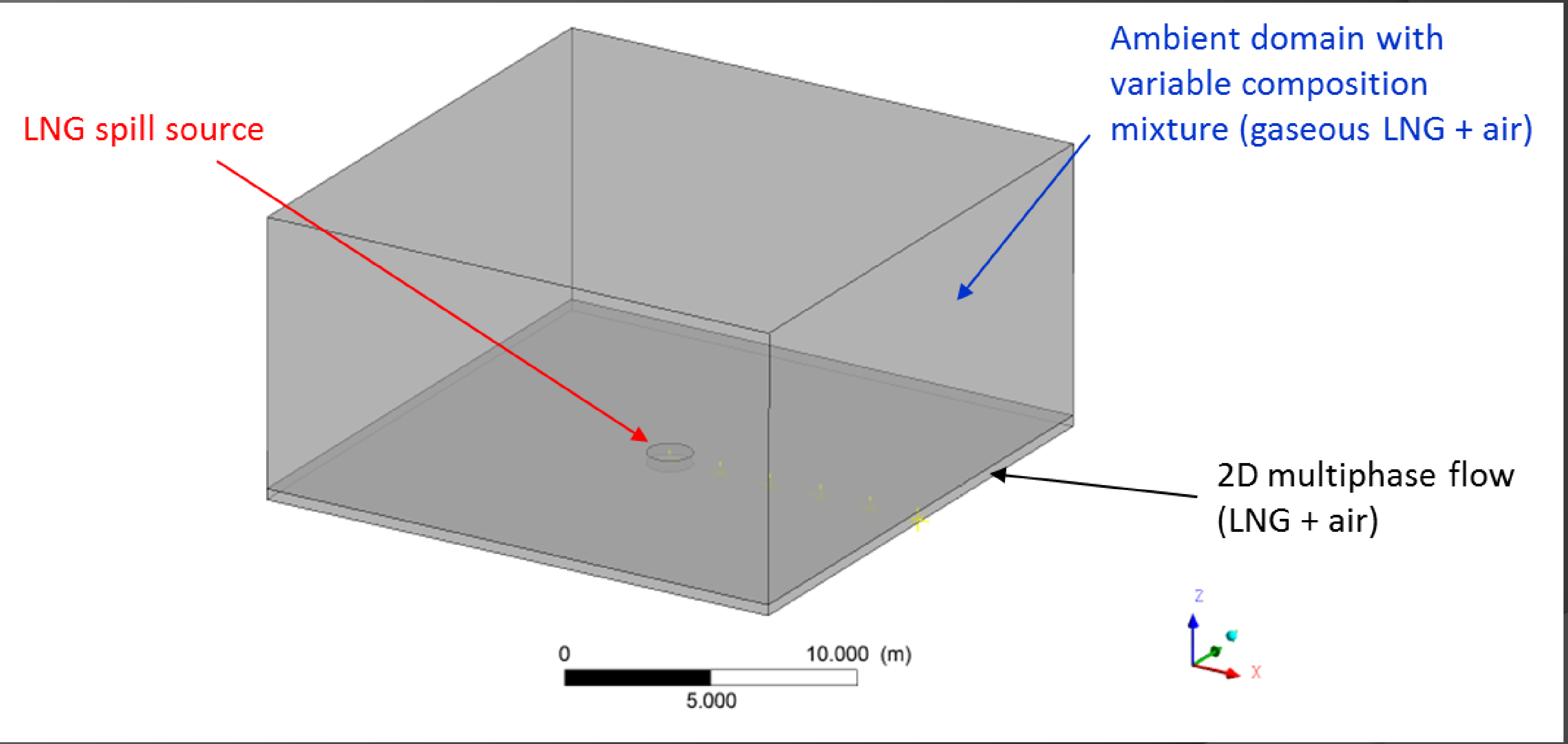

Liquid layer dynamics

Multiphase formulation of the liquid layer

→ applicable in most of general purpose CFD codes

- Definition of liquid fraction (r_{LNG}) in a 2D multiphase domain

$$h_{LNG} = r_{LNG} h_{layer}$$

- The rest of the 2D multiphase domain (1-r_{LNG}) occupied by entrained air

Liquid layer dynamics

Source approximation

- LNG release height (h_{rel}) determines the liquid velocity at the point of contact with water

$$u_{LNG@source} = \sqrt{2gh_{rel}}$$

- The initial point of a spreading LNG layer defined as a volumetric source with the diameter (d_{source})

$$r_{LNG@source} = \frac{\dot{m}_{LNG@rel}}{\rho_{LNG} u_{LNG@source} (0.25\pi d_{source}^2)}$$

It determines the LNG volume fraction of the source ($r_{LNG@source}$).

Liquid layer dynamics

Source approximation

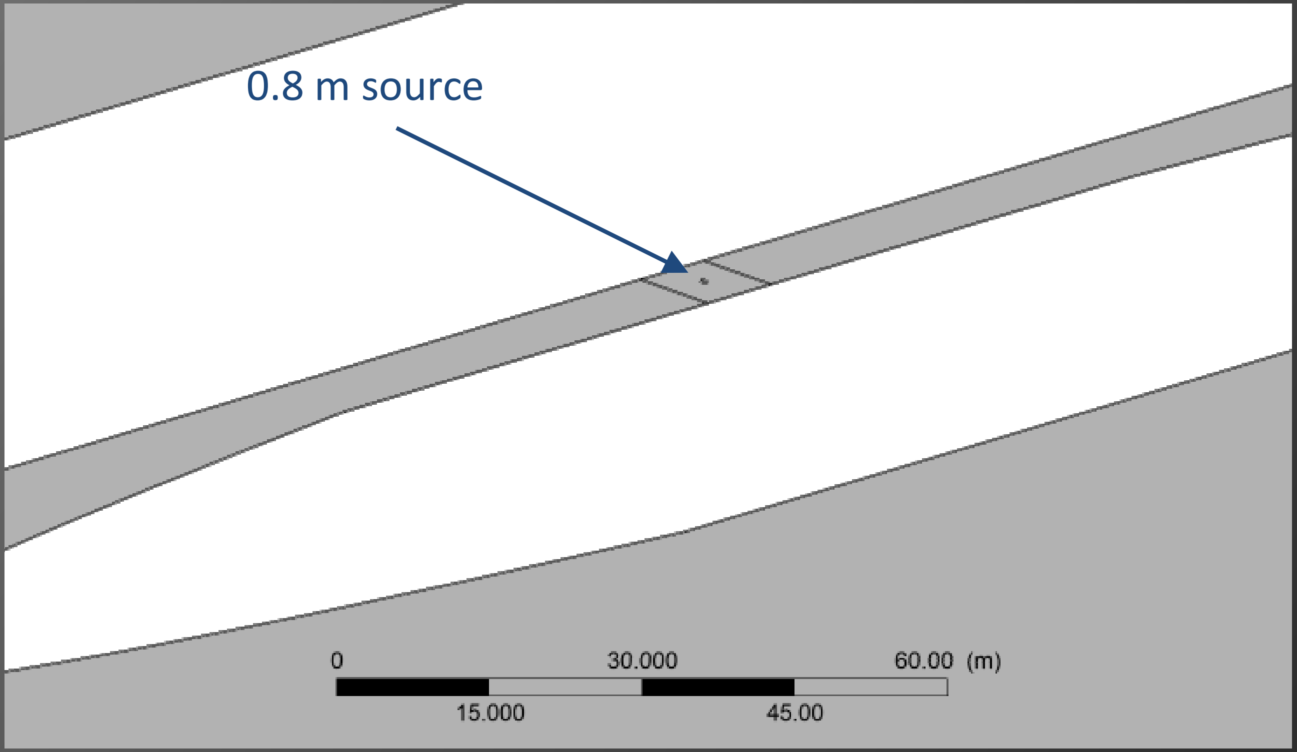

Location of the liquid layer source between two vessels

Liquid layer dynamics

Source approximation

- Preservation of kinetic energy:

$$u_{LNG@source} = \frac{\dot{m}_{LNG@rel}}{\rho_{LNG} r_{LNG@source} (0.25\pi d_{source}^2)} = \frac{\dot{m}_{LNG@rel}}{\rho_{LNG} r_{LNG@source} (\pi d_{source} h_{layer})}$$

- Definition of the appropriate height of the liquid layer simulation domain:

$$h_{layer} = 0.25 d_{source}$$

Liquid layer dynamics

Spreading of the liquid layer

- Multiphase formulation of the mass transport equation for LNG

$$\partial_t(\rho_{LNG} r_{LNG}) + \partial_i(\rho_{LNG} r_{LNG} u_i) = \frac{\dot{m}_{LNG@rel}}{h_{layer}(0.25\pi d_{source}^2)}$$

- Complimentary transport equation for the ambient air volume fraction

$$\partial_t(\rho_{amb} r_{amb}) + \partial_i(\rho_{amb} r_{amb} u_i) = \frac{\dot{m}_{LNG@rel}}{h_{layer}(0.25\pi d_{source}^2)}\left(\frac{\rho_{amb}}{\rho_{LNG}}\right)\left(\frac{1 - r_{LNG@source}}{r_{LNG@source}}\right)$$

For the presented model, the homogenous multi-phase formulation was selected.

Liquid layer dynamics

Spreading of the liquid layer

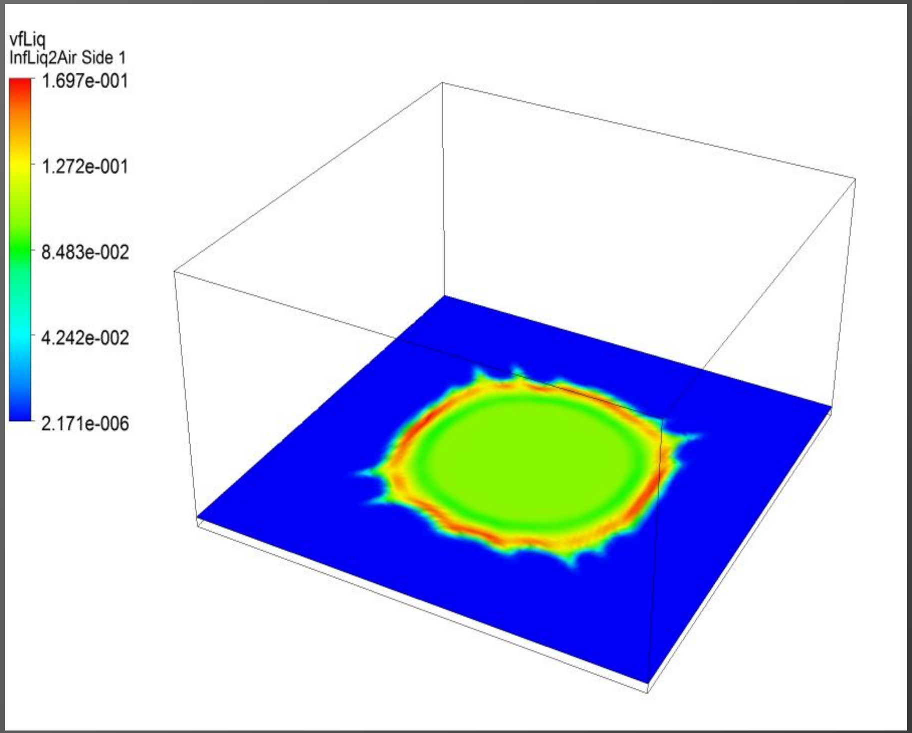

Liquid volume fraction distribution 20 s from the start of the release for one of the tests

Liquid layer dynamics

Domain interface exchange

Coupling between the liquid layer and the ambient domain via source terms:

- volumetric source terms in the 2D liquid layer domain
- interface source term in the ambient domain

Asymmetric approximation of mass exchange between the liquid layer and the ambient domain:

$$\partial_t(\rho_{LNG} r_{LNG}) + \partial_i(\rho_{LNG} r_{LNG} u_i) = \cdots - \frac{j_{evap}}{h_{layer}}$$

$$\partial_t(\rho_{amb} Y_k) + \partial_i(\rho_{amb} Y_k u_i) = \cdots + Y_k \frac{j_{evap}}{h_{layer}}$$

Liquid layer dynamics

Domain interface exchange

Sensitivity of the 2D liquid layer domain to mass source and sink terms

- compensation of volume outflow rate associated with LNG boiling
- source term for the ambient air volume fraction in the liquid domain

$$\partial_t(\rho_{amb} r_{amb}) + \partial_i(\rho_{amb} r_{amb} u_i) = \cdots + \frac{j_{evap}}{h_{layer}}\left(\frac{\rho_{amb}}{\rho_{LNG}}\right)$$

- source term for the momentum transport equation for the gaseous phase

$$\partial_t(\rho_{amb} r_{amb} u_j) + \partial_i u_i(\rho_{amb} r_{amb} u_j) = \cdots - (\rho_{amb} r_{amb} u_j)\frac{u_i}{h_{layer}} + (\rho_{amb} r_{amb} u_j)\frac{u_0}{h_{layer}}$$

These additional source terms are only required due to the multiphase formulation; they may not be required if the shallow water or VoF models are available.

Liquid layer dynamics

Domain interface exchange

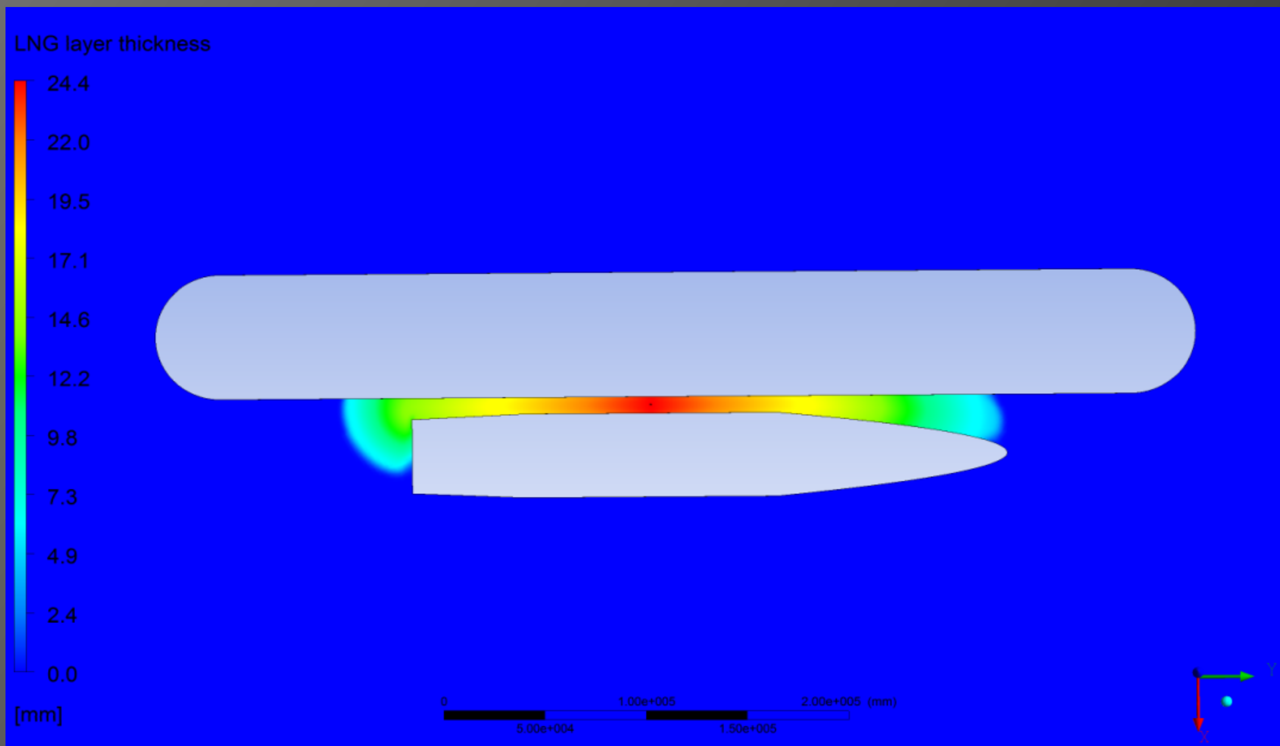

Results of a model test using a constant LNG evaporation mass flux j_{evap} of 0.2 kg/m^{2}s

Boiling regimes and RPT

LNG saturation temperature at atmospheric conditions is -162°C

$\rightarrow$ in contact with water it starts to boil

- evaporation mass flux (j_{evap}) in different LNG boiling regimes
- j_{evap} of 0.02 and 0.3 kg/m^{2}s have been recorded
- constant evaporation mass flux approximation and Rapid Phase Transition (RPT)
- introduction of different boiling regimes in the modelling procedure

Boiling regimes and RPT

Rapid Phase Transition (RPT) is the result of the LNG layer superheating

- instantaneous release of thermal energy when maximum superheating reached
- formation of a pressure wave

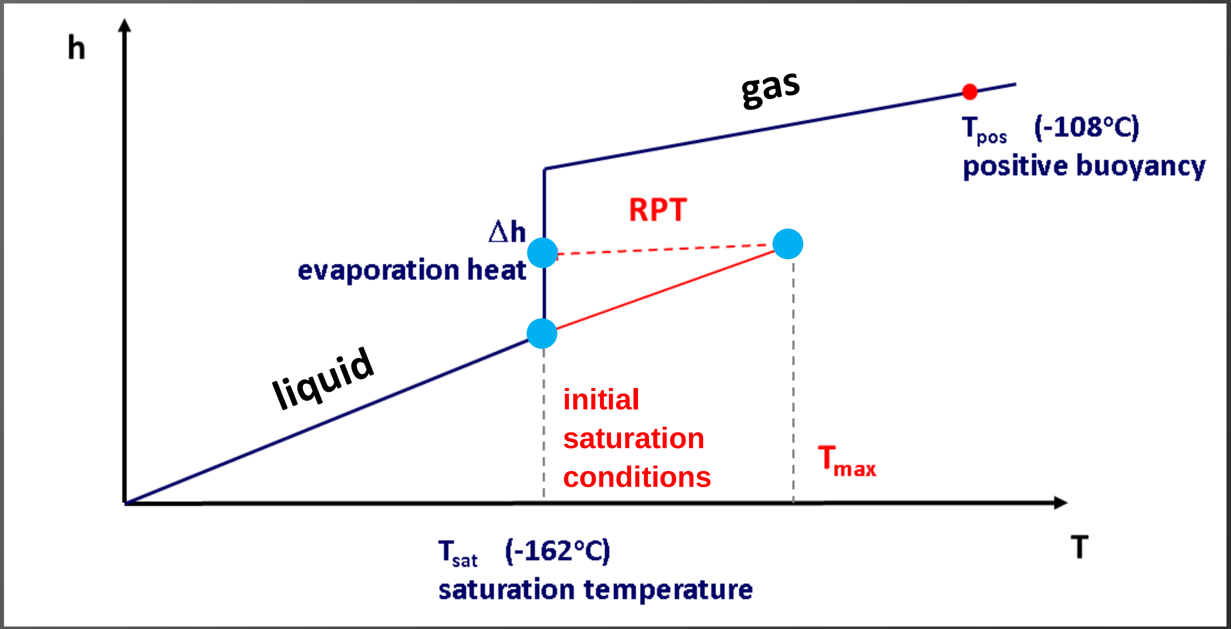

LNG temperature - enthalpy diagram with marked initial saturation conditions, super-heating, RPT and further heating of the gaseous LNG

Boiling regimes and RPT

Boiling diagram relates the temperature difference ($T_{water} - T_{LNG}$) with the resulting heat flux to the LNG layer (q_{evap})

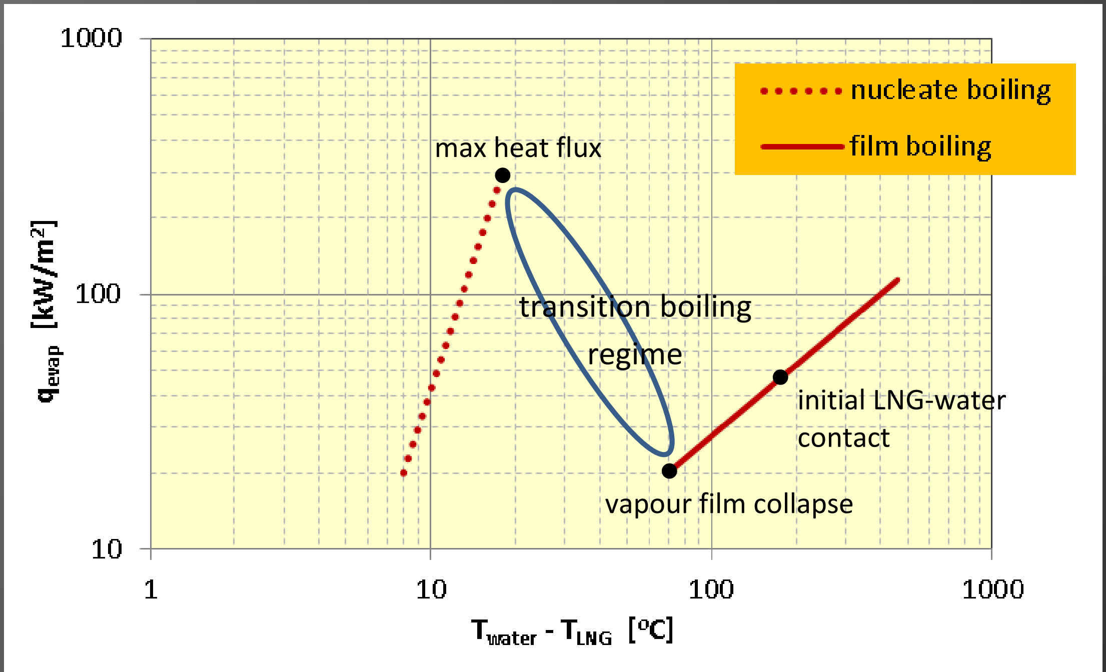

LNG boiling curve
(based on Sciance et al, 1967)

Based on the heat flux q_{evap}, the associated evaporation mass flux is

$$j_{evap} = \frac{q_{evap}}{\Delta h_{evap}}$$

Boiling regimes and RPT

Film boiling regime

Thermal state of the water surface is not directly included in the current model

$\rightarrow$ it needs to be approximated by an empirical correlation

- evaporation mass flux decreases with the contact time
- maximum j_{max} is at the point of the initial LNG jet impingement
- tracking and recording of the local contact time

$$\partial_t t_{cont} = H(r_{LNG}), \quad \text{where} \quad H(r_{LNG}) = \begin{cases} 1, r_{LNG} > \delta \\ 0, r_{LNG} \leq \delta \end{cases}$$

- evaporation mass flux in the film boiling regime (US Coast Guard, 1980)

$$j_{film} = j_{max} - At_{cont} \qquad \text{where} \quad j_{max} = 0.38 \, \frac{kg}{m^2 s} \ \text{and} \ A = 0.015 \, \frac{kg}{m^2 s}$$

Liquid layer dynamics

Film boiling regime

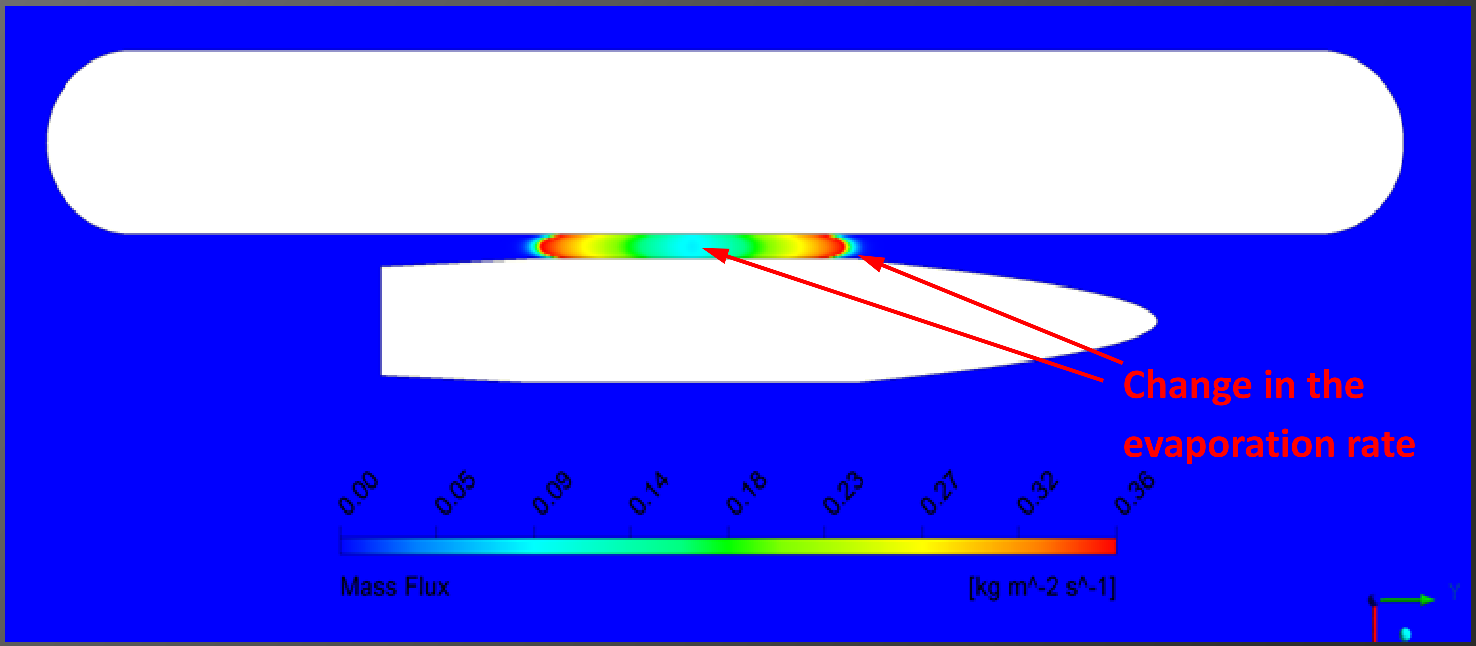

Contact time simulation test - evaporation mass flux between the vessels after 20 s

Boiling regimes and RPT

Transition boiling regime

Vapour film collapses when

$$(T_{water} - T_{LNG}) \leq 70 \text{ to } 80^{o}\text{C}$$

- direct contact between LNG and water surface
- lowest temperature difference determined by the surface temperature T_{water}
- film boiling regime curve & evaporation mass flux as a function of contact time $\rightarrow$ contact time (t_{crit}) to reach LNG boiling crises

$$t_{crit} = \frac{1}{A}\left(j_{max} - \frac{q_0}{\Delta h_{evap}}(\Delta T_{min}/1^{\circ}\text{C})^{0.923389}\right) \text{ , where } \Delta T_{min} = 80^{\circ}\text{C}$$

- $t > t_{crit} \rightarrow$ heat flux from water to the LNG layer increases to q_{max}

Boiling regimes and RPT

Transition boiling regime

- LNG evaporation utilises only a part of available heat transfer to LNG

$\Delta h_{evap} j_{max} < q_{max}$ where $q_{max} = 300 \frac{kW}{m^2}$ and $j_{max} = 0.38 \frac{kg}{m^2 s}$

- LNG layer superheating leading to an RPT event

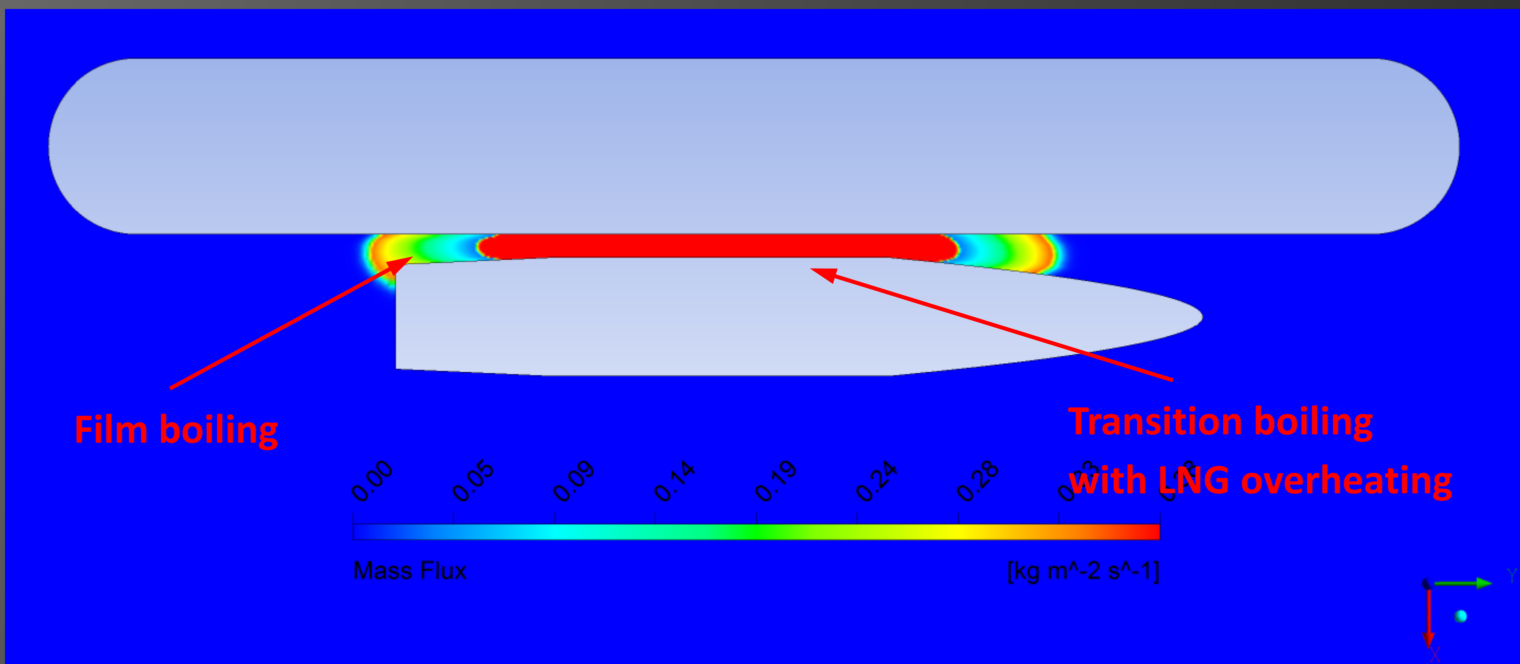

Transition boiling simulation test - evaporation mass flux between the vessels after 56 s

Boiling regimes and RPT

Rapid phase transition

Triggering of an RPT event when T_{LNG} reaches T_{max}

- T_{max} was set to 191 K as proposed by Melhem (2006) for a similar LNG composition
- sensible heat in the form of LNG superheating is released causing rapid evaporation

$$\partial_t(\rho_{LNG} r_{LNG}) + \partial_i(\rho_{LNG} r_{LNG} u_i) = \cdots - \frac{j_{RPT}}{h_{layer}}$$

$$\partial_t\left(\rho_{LNG} r_{LNG} h_{super}\right) + \partial_i\left(\rho_{LNG} r_{LNG} u_i h_{super}\right) = \cdots - \frac{j_{RPT}}{h_{layer}}\left(\Delta h_{evap}\right)$$

where $h_{super} = c_p(T_{LNG} - T_{sat})$

- evaporation mass flux limited by sonic speed of the surrounding gas

$$j_{RPT} = \rho_{gas} c_{gas} \quad \text{where} \quad c_{gas} = \sqrt{\gamma R T_{sat}}$$

Boiling regimes and RPT

Rapid phase transition

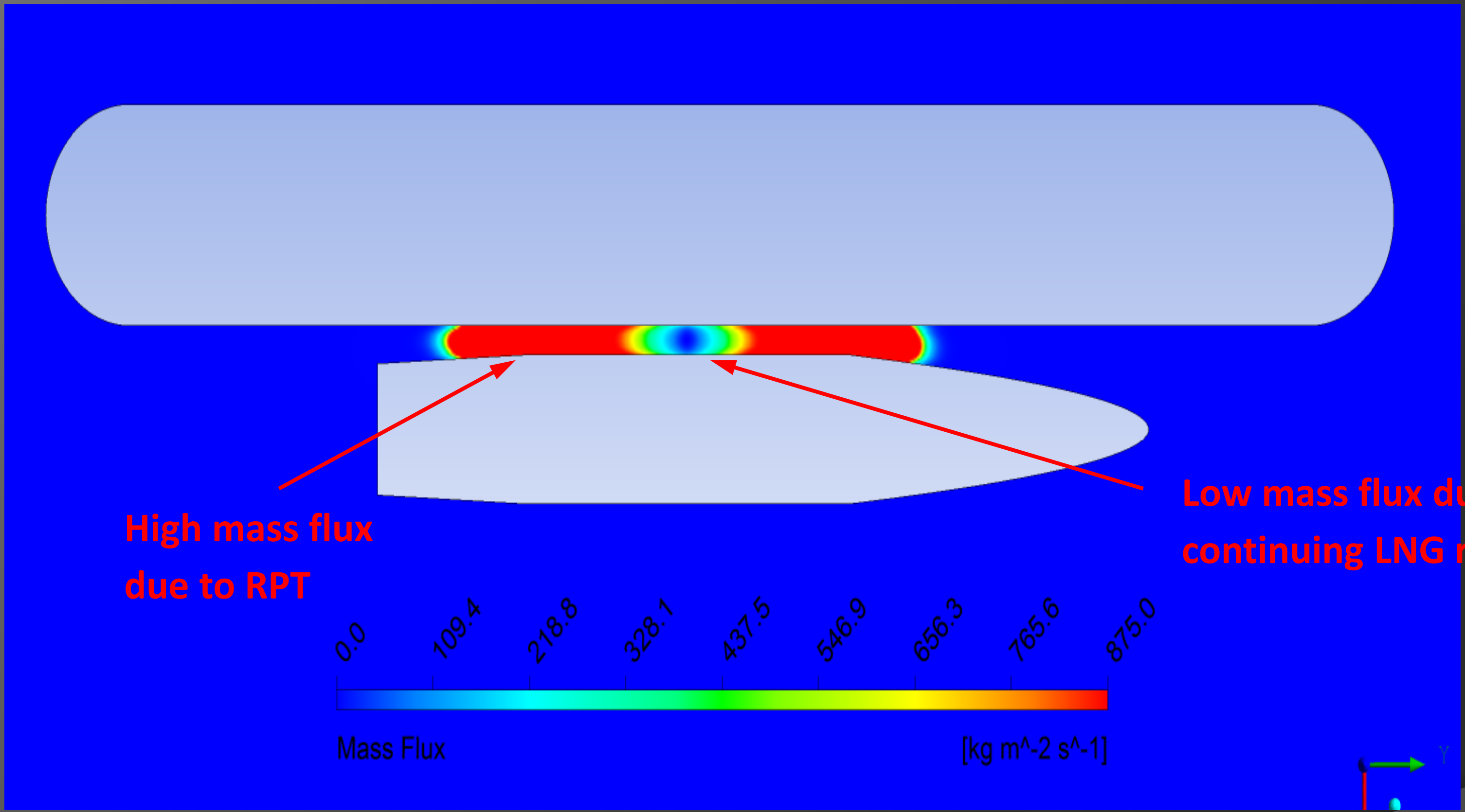

RPT simulation test - evaporation mass flux between the vessels after 55.4 s

Boiling regimes and RPT

Nucleate boiling

- LNG superheating (h_{super}) decrease to zero $\rightarrow$ RPT concludes
- remaining LNG is well mixed with water $\rightarrow$ nucleate boiling regime
- small temperature difference $\rightarrow$ direct contact between LNG and water
- maximum evaporation mass flux (j_{max})

Dispersion

- Transfer of evaporation mass flux from the liquid layer to the gaseous ambient domain

$$\partial_t(\rho_{amb} Y_k) + \partial_i(\rho_{amb} Y_k u_i) = \cdots + Y_k \frac{j_{evap}}{h_{layer}}$$

- Dispersion of gaseous LNG by the imposed wind velocity field

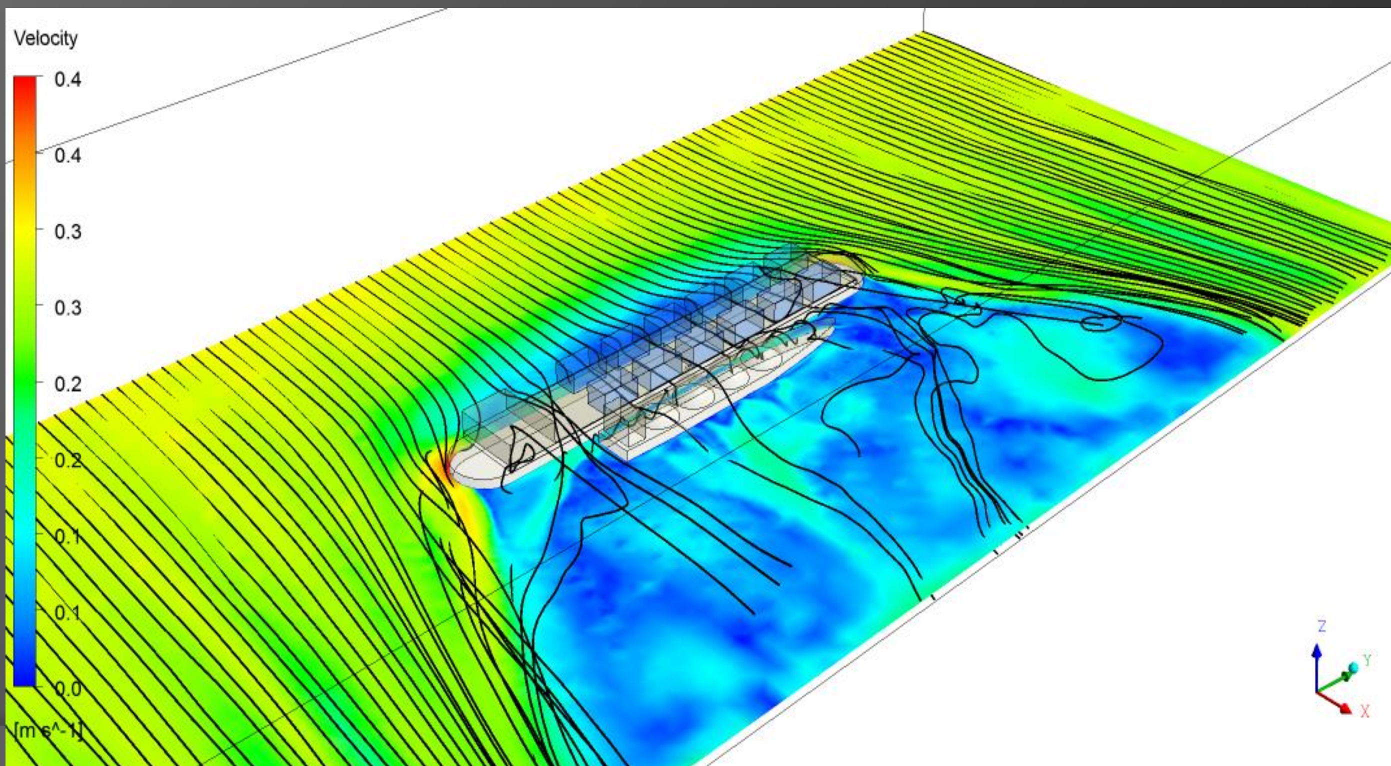

Imposed initial velocity field due to cross-wind

Dispersion

Dispersion of gaseous LNG cloud mostly depends on its buoyancy

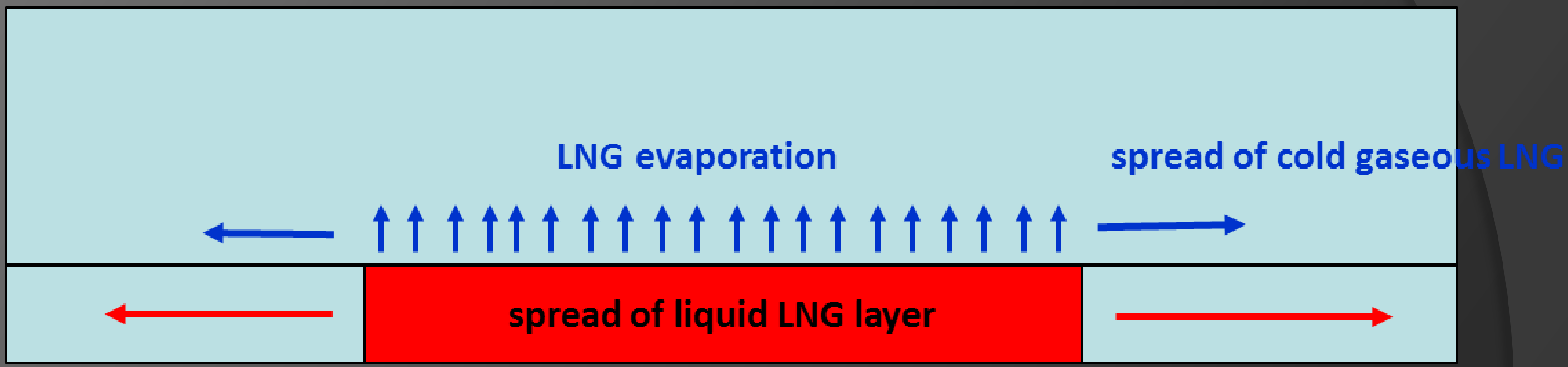

- initially, negatively buoyant gaseous LNG
- freely flows above the water surface due to higher density
- cloud needs to heat-up above -108°C to become positively buoyant
- cloud lift-off strongly enhances its dispersion

Dispersion

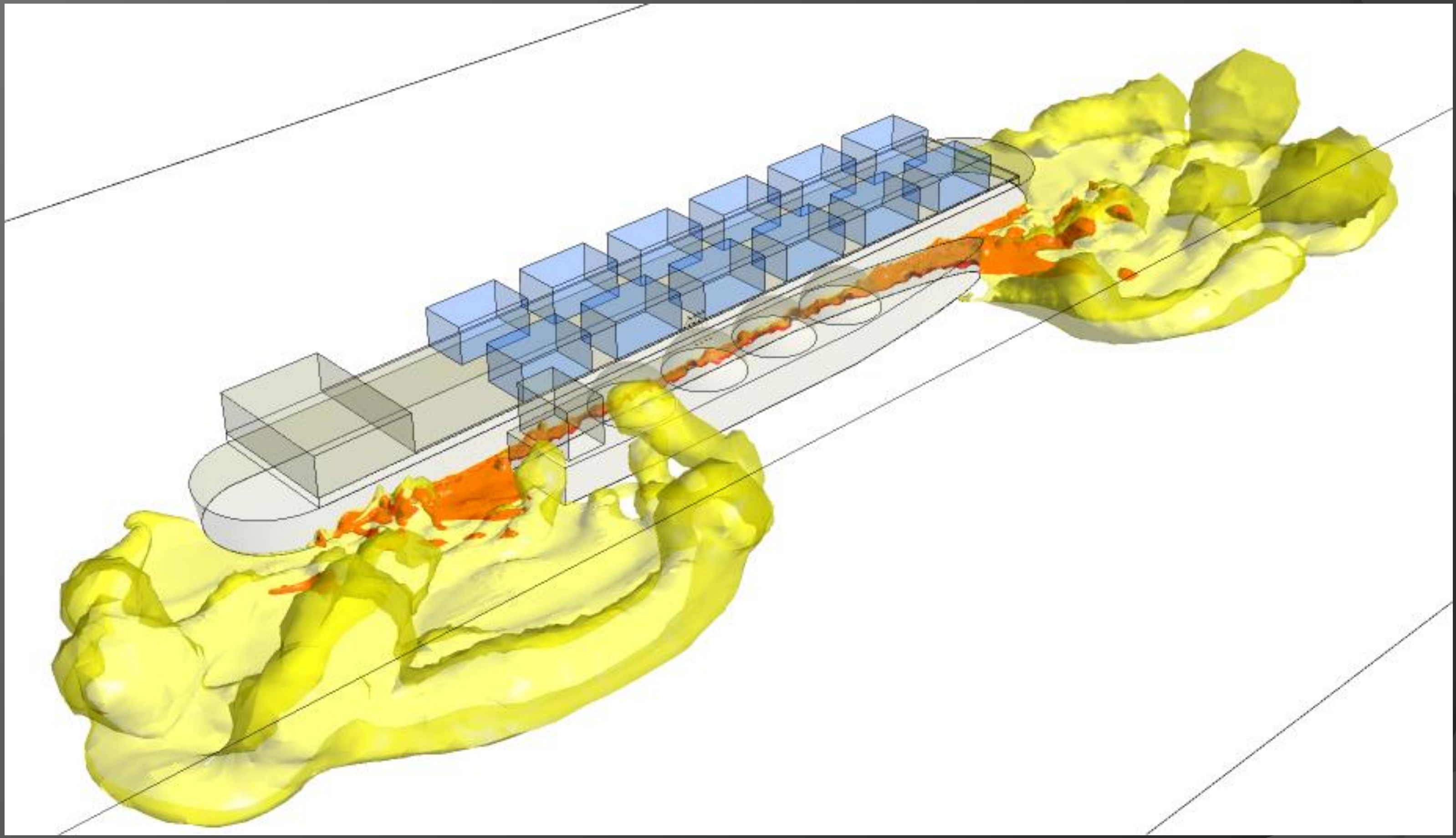

Dispersing cloud of gaseous LNG (1 and 10% mass fraction isosurfaces) after 320 s

CFD simulation results and discussion

Presentation of CFD results only for the process train release case

Two main objectives

- volume of the flammable cloud and its distribution
- overpressure approximation due to RPT

CFD simulation results and discussion

Flammability limits and volume of the cloud

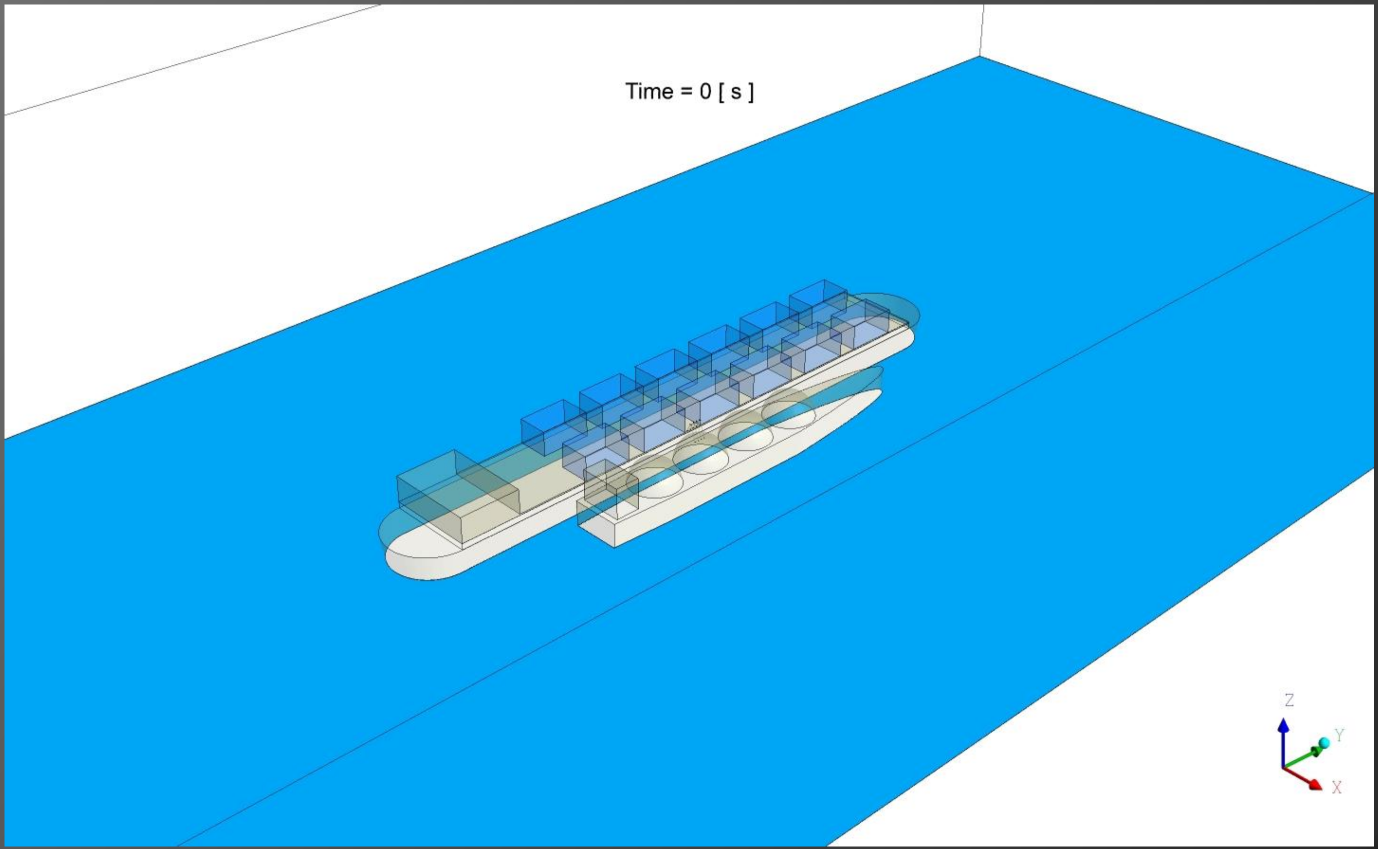

Lower (4.5%) and upper (15%) flammability limit of gaseous LNG at 25^{o}C

CFD simulation results and discussion

Flammability limits and volume of the cloud

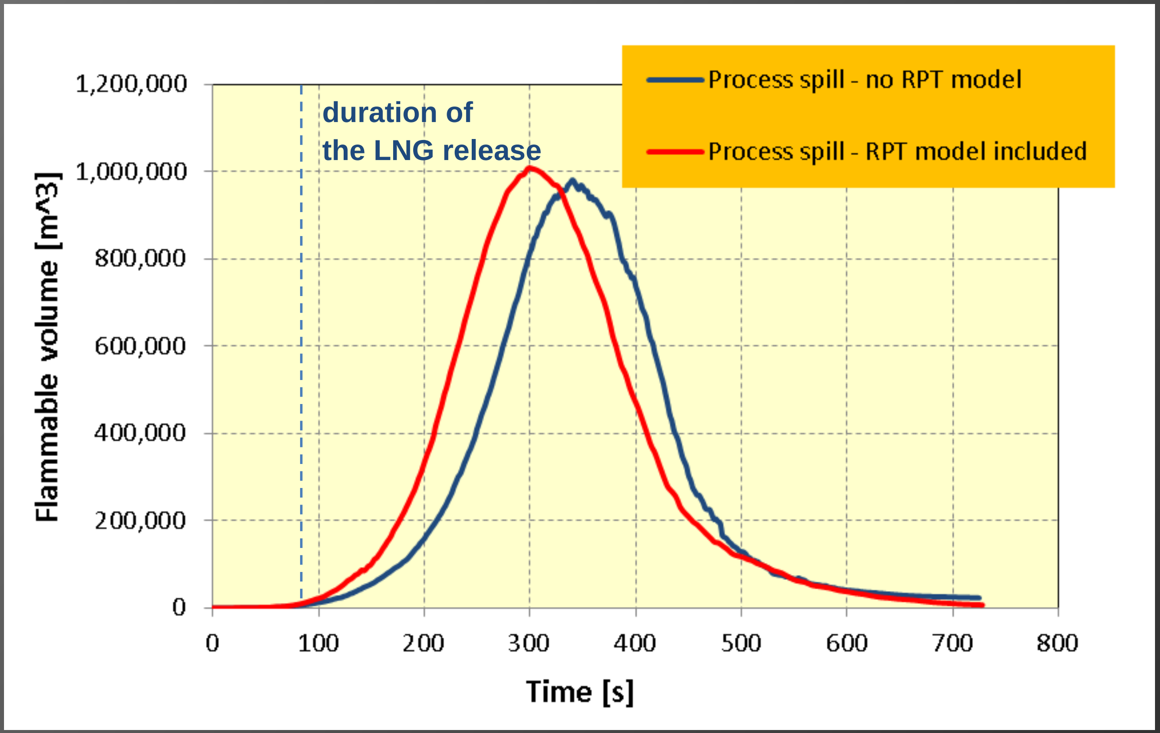

Time variation of the gaseous LNG flammable volume

- LNG remains present between both vessels longer
- negative buoyancy of the gaseous LNG and the time required for the cloud lift-off

CFD simulation results and discussion

Overpressure approximation

- LNG layer superheating constrains an RPT event
- small amount of LNG involved $\rightarrow$ effect on the dispersion process is limited
- formation of a pressure wave

CFD simulation results and discussion

Overpressure approximation

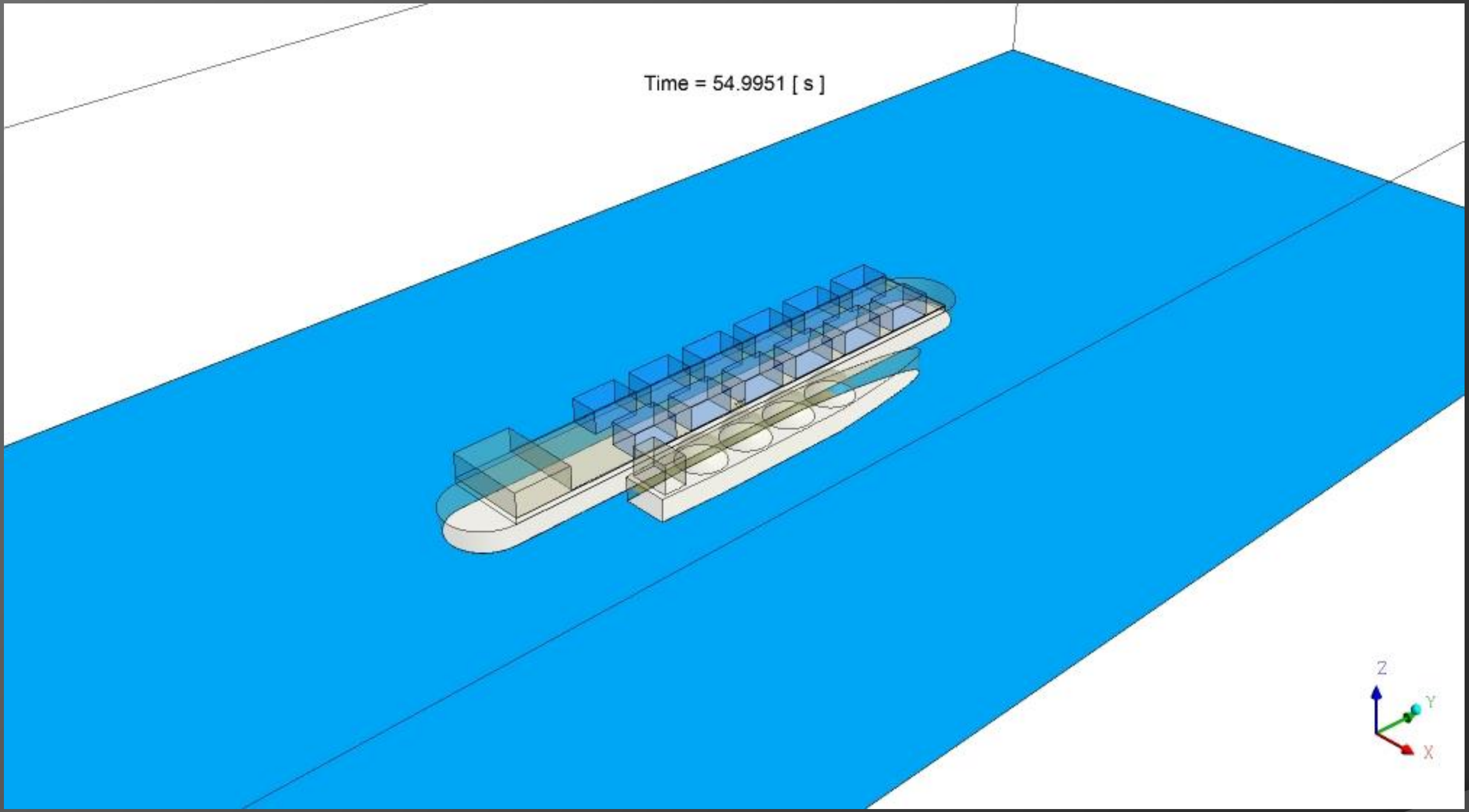

Pressure wave after the RPT event – overpresure isosurface of 400 Pa

CFD simulation results and discussion

Overpressure approximation

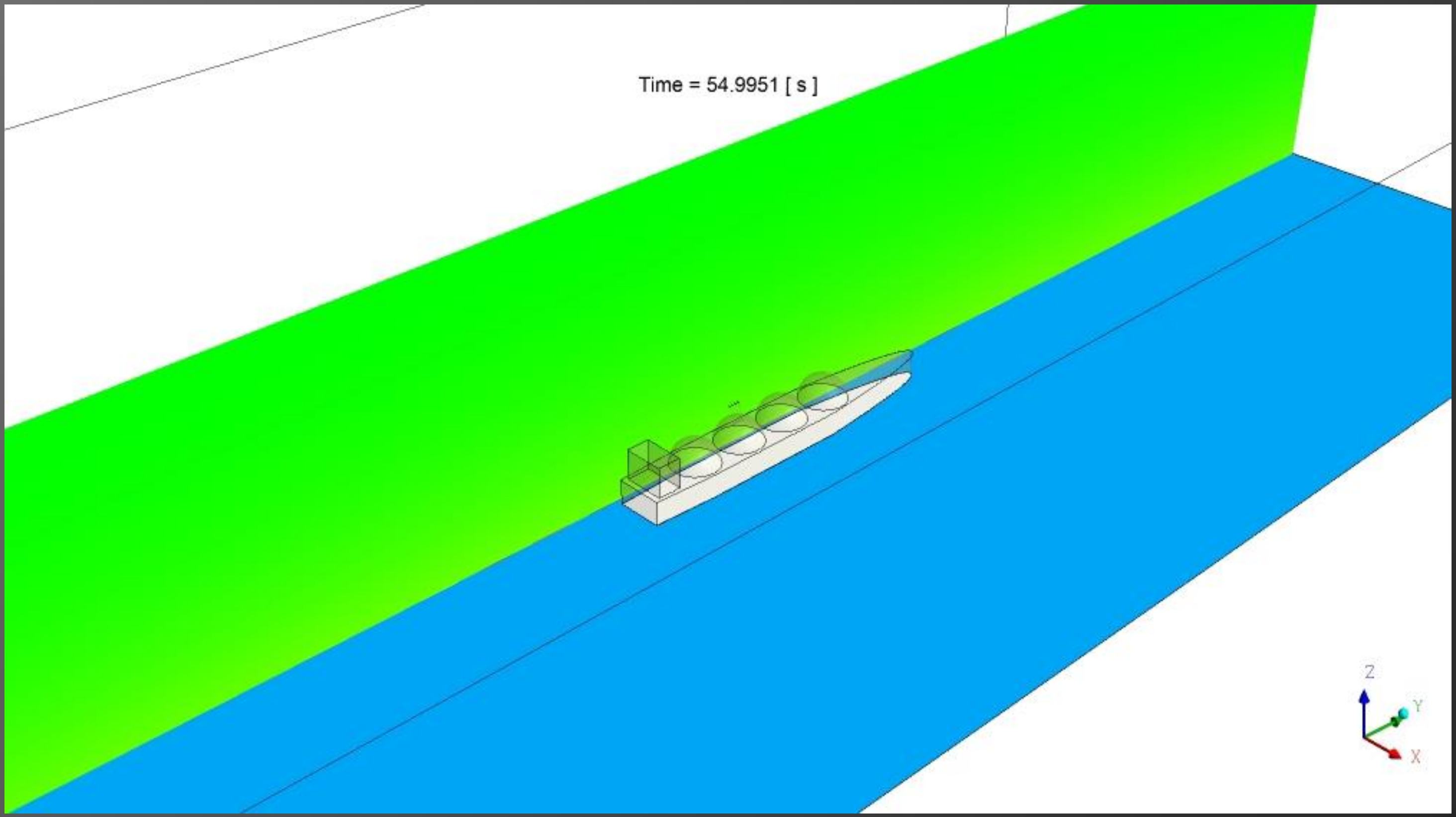

Cross-section of the over-pressure field ($-2\ \mathrm{kPa} \leq \Delta p \leq 2\ \mathrm{kPa}$) after the RPT event

CFD simulation results and discussion

Overpressure approximation

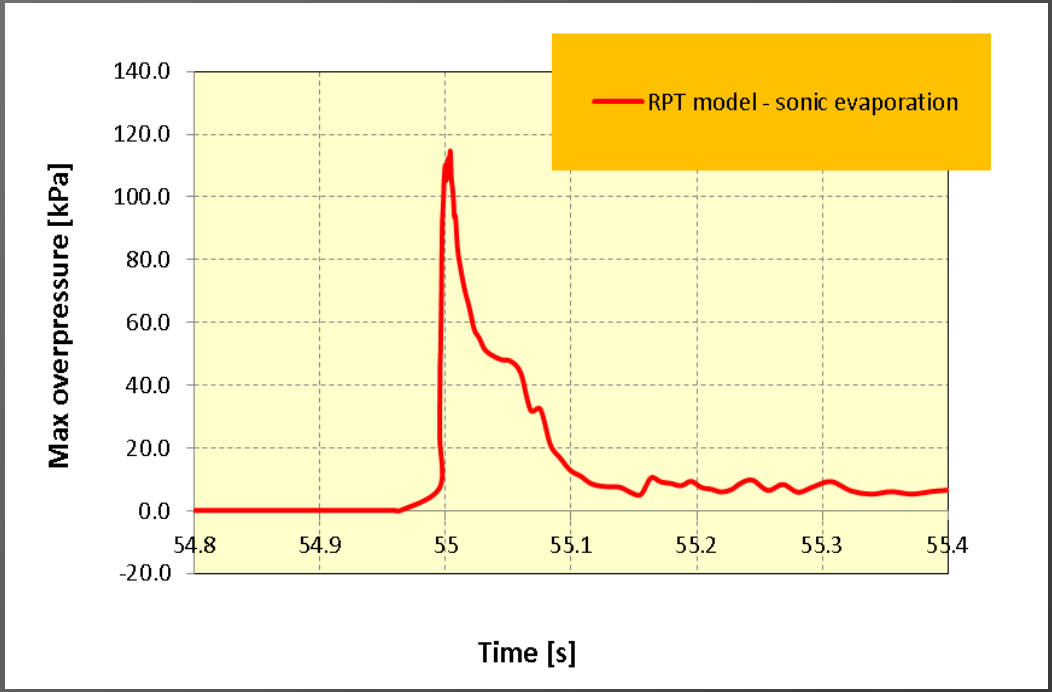

Time variation of the maximum overpressure during the RPT event

- maximum overpressure exceeds 110 kPa
- pressure peaks occur close to the water surface with temperatures near -162°C
- combination of high pressures and extremely low temperatures

→ significant risk of structural failure

Further challenges and conclusions

- generic approach that can be used in most CFD codes with multiphase flow capabilities
- many modelling simplifications especially in formulating the effects of different boiling regimes
- incomplete data as only a single source for the boiling curve definition is available
- energy transport equation in modelling the LNG liquid layer and quantification of heat transfer between the water and the liquid layer

Further challenges and conclusions

- CFD simulation of the FLNG process train failure to demonstration the capability of the developed methodology
- estimate the size and behaviour of the flammable cloud generated by the LNG spill
- horizontal spread of the flammable cloud due to negative buoyancy and reduction of fire related risk
- overpressure due to an RPT event exceeds 110 kPa
- risk of structural failure due to high pressure loading at low temperatures (-162^{o}C)

Need for further parametric studies to determine sensitivity of RPT events and their consequences!

Thank you !

Contact information

Dr Andrei Horvat

Phone: +44 1235 819 729

Mobile: +44 79 72 17 27 00

Skype: a.horvat

E-mail: mail@caspus.co.uk

Web: www.caspus.co.uk

References

1. G.A. Melhem, S. Saraf & H. Ozog, Understand LNG Rapid Phase Transitions (RPT), ioMosaic Corporation, 2006.
2. E.M. Drake, A.A. Jeje & R.C. Reid, Transient boiling of liquefied cryogens on a water surface: I. Nitrogen, methane and ethane, Int. J. Heat Mass Transfer, 1975, Vol. 18, pp. 1361-1368.
3. E.M. Drake, A.A. Jeje & R.C. Reid, Transient boiling of liquefied cryogens on a water surface: II. Light hydrocarbon mixture, Int. J. Heat Mass Transfer, 1975, Vol. 18, pp. 1369-1375.
4. H.K. Kytömaa and T.L. Morse, Variations in the evaporation rate of a cryogenic liquid on a water surface, 2010 Int. Sym., Beyond Regulatory Compliance, Making Safety Second Nature, Oct. 26-28, 2010, Hilton College Station Conference Center, College Station, Texas, USA.
5. P. Cleaver, M. Johnson & B. Ho, A summary of some experimental data on LNG safety, J. Hazardous Materials, 2007, Vol. 140, pp. 429-438.

References

6. A. Luketa-Hanlin, A review of large-scale LNG spills: Experiments and modeling, J. Hazardous Materials, 2006, Vol. A132, pp. 119-140.
7. P.J. Waite, R.J. Whitehouse, E.B. Winn & W.A. Wakeham, The spread and vaporisation of cryogenic liquids on water, J. Hazardous Materials, 1983, Vol. 3, pp. 165-184.
8. D.M. Webber, S.E. Grant, M.J. Ivings, S.F. Jagger, LNG source term models for hazard analysis - A review of the state-of-the-art and an approach to model assessment, RR789 Health and Safety Laboratory, 2010.
9. D.W. Hissong, Keys to modeling LNG spills on water, J. Hazardous Materials, 2007, Vol. 140, pp. 465-477.
10. F. Gavelli, E. Bullister & H. Kytomaa, Application of CFD (Fluent) to LNG spills into geometrically complex environments, J. Hazardous Materials, 2008, Vol. 159, pp. 158-168.

References

11. F. Gavelli, S.G. Davis & O.R. Hansen, A unified model for LNG pool spread and vapor dispersion: Is wind scooping really a factor? American Institute of Chemical Engineers, 2010 Spring Meeting, 10th Topical Conference on Gas Utilization, March 24, 2010, San Antonio, Texas, USA.
12. J.A. Fay, Model of spills and fires from LNG and oil tankers, J. Hazardous Materials, 2003, B96, pp. 171-188.
13. P.K. Raj, LNG fires: a review of experimental results, models and hazard prediction challenges, J. Hazardous Materials, 2007, 140, pp. 444-464.
14. B. Sun, R.P. Utikar, V.K. Pareek, K. Guo, Computational fluid dynamics analysis of liquefied natural gas dispersion for risk assessment strategies. J. Loss Prev. Process Ind., 2013, 26, pp. 117–128.
15. B. Sun, K. Guo, V.K. Pareek, Computational fluid dynamics simulation of LNG pool fire radiation for hazard analysis, J. Loss Prev. Process Ind., 2014, 29, pp. 92–102.
16. B. Sun, K. Guo, V.K. Pareek, Dynamic simulation of hazard analysis of radiations from LNG pool fire, J. Loss Prev. Process Ind., 2015, 35, pp. 200–210.

References

17. B. Sun, K. Guo, V.K. Pareek, Hazardous consequence dynamic simulation of LNG spill on water for ship-to-ship bunkering, Process Safety and Environmental Protection, 2017, 107, pp. 402–413.

18. O.R. Hansen, M. Ichard & S.G. Davis, Validation of FLACS for vapor dispersion from LNG Spills: Model evaluation protocol, 12th Annual Symposium, Mary Kay O'Connor Process Safety Center, October 27-28, 2009, Texas A&M University, College Station, Texas, USA, pp. 712-743.

19. Ansys Inc, Fluent Rel. 18.0, User Manual, Section 17.3 - Volume of Fluid (VOF) model theory.

20. G.-M. Wuersig, J. Gaughan, B. Scholz, L. Sannes, S. Kabelac, A. Leder, Effects of enveloping pool fires on LNG tank containment systems, May 25 – 28, 2009, GasTech, Abu-Dhabi.

21. C.T. Sciance, C.P. Colver, C.M. Sliepcevich, Pool boiling of methane between atmospheric pressure and the critical pressure, Advances in Cryogenic Engineering, Vol. 12, Jan. 1967.

References

22. Panel on Liquefied Natural Gas Safety Evaluation, Safety Aspects of Liquefied Natural Gas in the Marine Environment, Report NMAB-354, United States Coast Guard, 1980, p. 274.

23. www.ansys.com/products/fluids/ansys-cfx, accessed 2017/04/13.